APL Photonics

Witnessing entangled two-photon absorption via quantum interferometry

Cite as: APL Photonics **8**, 036104 (2023); https://doi.org/10.1063/5.0128249
Submitted: 27 September 2022 • Accepted: 12 February 2023 • Published Online: 07 March 2023

Áulide Martínez-Tapia, Samuel Corona-Aquino, Freiman Triana-Arango, et al.

APL Photonics ARTICLE scitation.org/journal/app

Witnessing entangled two-photon absorption via quantum interferometry

Cite as: APL Photon. 8, 036104 (2023); doi: 10.1063/5.0128249
Submitted: 27 September 2022 • Accepted: 12 February 2023 •
Published Online: 7 March 2023

View Online Export Citation CrossMark

Áulide Martínez-Tapia,[1] Samuel Corona-Aquino,[1] Freiman Triana-Arango,[2] Chenglong You,[3] Rui-Bo Jin,[4] Omar S. Magaña-Loaiza,[3] Shi-Hai Dong,[5,6,a)] Alfred B. U'Ren,[1,a)] and Roberto de J. León-Montiel[1,a)]

AFFILIATIONS

[1] Instituto de Ciencias Nucleares, Universidad Nacional Autónoma de México, Apartado Postal 70-543, 04510 CDMX, Mexico
[2] Centro de Investigaciones en Optica AC, Apartado Postal, 37150 Leon, Gto, Mexico
[3] Quantum Photonics Laboratory, Department of Physics and Astronomy, Louisiana State University, Baton Rouge, Louisiana 70803, USA
[4] Hubei Key Laboratory of Optical Information and Pattern Recognition, Wuhan Institute of Technology, Wuhan 430205, China
[5] Research Center for Quantum Physics, Huzhou University, Huzhou 313000, China
[6] Laboratorio de Ciencias de la Informacion Cuantica, CIC, Instituto Politecnico Nacional, UPALM, C.P. 07700 CDMX, Mexico

[a)] **Authors to whom correspondence should be addressed:** dongsh2@yahoo.com; alfred.uren@correo.nucleares.unam.mx; and roberto.leon@nucleares.unam.mx

ABSTRACT

Recent investigations have suggested that the use of non-classical states of light, such as entangled photon pairs, may open new and exciting avenues in experimental two-photon absorption spectroscopy. Despite several experimental studies of entangled two-photon absorption (eTPA), there is still a heated debate on whether eTPA has truly been observed. This interesting debate has arisen mainly because it has recently been argued that single-photon-loss mechanisms, such as scattering or hot-band absorption, may mimic the expected entangled-photon linear absorption behavior. In this work, we focus on transmission measurements of eTPA and explore three different two-photon quantum interferometers in the context of assessing eTPA. We demonstrate that the so-called N00N-state configuration is the only one among those considered insensitive to linear (single-photon) losses. Remarkably, our results show that N00N states may become a potentially powerful tool for quantum spectroscopy, placing them as a strong candidate for the certification of eTPA in an arbitrary sample.

I. INTRODUCTION

Nonlinear spectroscopy techniques have been shown to constitute a powerful tool for extracting information about the energy dynamics and chemical structure of unknown substances and molecules.[1–4] As such, they have played a fundamental role in the development of technologies used in modern society, from process control and manufacturing to pollution monitoring, also including homeland security and healthcare.[5] While in the optical regime, these techniques are typically implemented by means of laser light, recent work has suggested that the use of non-classical light, such as entangled photon pairs, may offer new and exciting avenues for spectroscopy.[6–10]

The time- and frequency-correlations of entangled photon pairs have enabled the observation of non-trivial two-photon absorption phenomena, such as the linear dependence of two-photon absorption rate on the photon flux.[11–13] These correlations have further been used for theoretically predicting effects such as two-photon-induced transparency,[14,15] induction of disallowed atomic transitions,[16] manipulation of quantum pathways of matter,[17–21] and control of molecular processes.[22,23] The linear dependence of two-photon absorption as a function of incident photon flux has been particularly attractive because it suggests that one may effectively excite nonlinear phenomena at much lower photon fluxes when compared to classical alternatives.[24]

During the past decade, entangled two-photon absorption spectroscopy has been identified as a promising tool for extracting the information about the electronic levels that contribute to the two-photon excitation of a molecular sample.[25–39] Moreover, it has been argued that it might provide a new route for probing broadband multi-photon processes with low-power, continuous-wave, single-frequency laser sources.[24] Although there is a lively debate on the true quantum enhancement that such a technique might offer for spectroscopy,[40–44] the experimental demonstration of its working principle, the so-called entangled two-photon absorption (eTPA), has recently become a topic of keen interest.[45–50] Indeed, it has been argued that the behavior in most of the reported experimental data so far may, in fact, be due to single-photon-loss phenomena, such as hot-band absorption[43] or scattering,[44] which might mimic the sought-after eTPA signals.

Consequently, a large group of physicists, chemists, and biologists has devoted considerable efforts to developing novel experimental schemes and metrics for certifying true eTPA. Some authors have relied on the linear to quadratic transition in the two-photon absorption rate as a function of incident photon flux.[47] Others have proposed new metrics based on single- and two-photon coincidence measurements, which make use of Hong–Ou–Mandel (HOM)-like interferometers.[44,49,51] In this work, we explore, in the context of eTPA, a number of two-photon quantum interferometry systems, leading to our demonstration that, among them, the so-called N00N-state configuration is the only one insensitive to single-photon losses. Our results show that, in transmission eTPA measurements, this N00N-state configuration is an ideal candidate for the true certification of entangled two-photon absorption. More importantly, and in contrast to other quantum-technology schemes in which N00N states are not typically robust,[52,53] our findings show that N00N states could play an important role in quantum spectroscopy.

II. RESULTS

A. Two-photon absorption measurements

In a typical eTPA transmission experiment, pairs of correlated photons, typically produced by spontaneous parametric downconversion (SPDC), interact with an arbitrary sample [see Fig. 1(a)]. The incident photon pairs are expected to drive a two-photon transition so that some pairs can be absorbed and, therefore, removed from the light beam traversing the sample. In most experiments,[30,44,49] the configuration shown in Fig. 1(b) is used to monitor, through coincidence measurements, the reduced photon-pair flux. Although one might be tempted to think that any pair-loss must be due to eTPA, it has been shown that single-photon-loss mechanisms, such as scattering[44] and hot-band absorption,[43] can lead to a similar behavior as would be expected for eTPA.[49] In view of this, it naturally becomes desirable to find a new, single-photon-loss insensitive photon-pair measurement scheme that enables direct certification of eTPA.

In order to assess the possible candidates for eTPA certification, we study and compare three distinct two-photon quantum interferometers, namely single-port and two-port Hong–Ou–Mandel setups and a N00N-state configuration. The three configurations are shown schematically in Figs. 1(b)–1(d), respectively. Note that the N00N state configuration makes use of a superposition of both photons impinging on input port a and both photons impinging on input port b of the BS. Possible experimental implementations for each of these configurations are discussed in detail in the supplementary material. In all configurations, two-photon interference takes place via a beam splitter (BS), which, for the sake of completeness, is

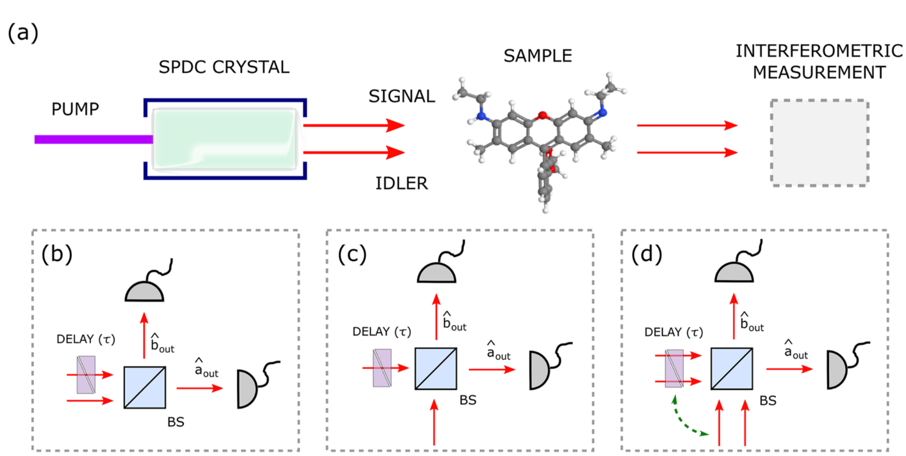

FIG. 1. Conceptual sketch of a typical eTPA transmission experiment. (a) Photon pairs, produced by spontaneous parametric downconversion (SPDC), interact with an arbitrary sample that experiences a two-photon absorption process, along with other single-photon-loss events. The attenuated photon-pair beam is then probed by means of an interferometric coincidence-detection scheme. In previous eTPA experiments,[30,44,49] pair losses due to eTPA have been monitored by means of the (b) single-port configuration, where a controllable delay τ is introduced in the path of one of the photons before it impinges on a lossless 50:50 beamsplitter (BS). Other possible interferometric configurations are the (c) two-port configuration, which describes a Hong–Ou–Mandel (HOM) interferometer, and (d) a N00N-state interferometer. Note that the photon pairs in panels (c) and (d) require additional optical elements (not shown) before reaching the BS. These are discussed in detail in the supplementary material.

assumed for the analysis below to exhibit losses. The input–output transformation of a lossy BS is given by[54]

$$\hat{a}_{\text{out}} = t(\omega)\hat{a}_{\text{in}}(\omega) + r(\omega)\hat{b}_{\text{in}}(\omega) + \hat{F}_a(\omega), \tag{1}$$

$$\hat{b}_{\text{out}} = t(\omega)\hat{b}_{\text{in}}(\omega) + r(\omega)\hat{a}_{\text{in}}(\omega) + \hat{F}_b(\omega), \tag{2}$$

with $\hat{a}_{\text{in,out}}(\omega)$ and $\hat{b}_{\text{in,out}}(\omega)$ depicting the input and output field modes of the BS, respectively. $r(\omega)$ and $t(\omega)$ are the BS reflection and transmission coefficients, while $\hat{F}_a(\omega)$ and $\hat{F}_b(\omega)$, which commute with the input field operators, are the Langevin noise operators associated with the BS losses.[54] Note that the Langevin operators lead to reflection and transmission coefficients that do not conserve energy, i.e., $|r(\omega)|^2 + |t(\omega)|^2 \le 1$.[54]

We can use Eqs. (1) and (2) to monitor the number of photon pairs that impinge on the BS by measuring the photon-coincidence rate at the output of the lossy BS. This can be expressed as

$$R = P(1_a, 1_b) = \langle \hat{N}_a \hat{N}_b \rangle, \tag{3}$$

where $\langle \cdots \rangle$ denotes an expectation value and the continuum number operators[55] for the two output ports are given by $\hat{N}_a = \int d\omega \hat{a}^\dagger_{\text{out}}(\omega)\hat{a}_{\text{out}}(\omega)$ and $\hat{N}_b = \int d\omega \hat{b}^\dagger_{\text{out}}(\omega)\hat{b}_{\text{out}}(\omega)$. Note that Eq. (3) is valid in the case of temporally isolated photon pairs, that is when the probability of two pairs being present within the two-photon correlation time is much lower than one. This is the typical situation in most of the recent eTPA experiments.[46–50]

By considering the simplest case of a lossless 50:50 BS, with $t = \pm ir$, where the i represents the $\pi/2$ phase difference between the transmitted and reflected beams, and $|t| = |r| = 1/\sqrt{2}$, we can readily find that the photon-coincidence rate for each of the above configurations (see the supplementary material and Ref. 56 for details) is given by

$$\begin{aligned} R_\pm(\tau) = \frac{1}{4}\int d\Omega_s d\Omega_i \Big[&|\phi(\Omega_s,\Omega_i)|^2 + |\phi(\Omega_i,\Omega_s)|^2 \pm \phi(\Omega_s,\Omega_i) \\ &\times \phi^*(\Omega_i,\Omega_s) e^{-i(\Omega_i-\Omega_s)\tau} \pm \phi^*(\Omega_s,\Omega_i)\phi(\Omega_i,\Omega_s) \\ &\times e^{i(\Omega_i-\Omega_s)\tau} \Big], \end{aligned} \tag{4}$$

$$\begin{aligned} R_N(\tau) = \frac{1}{4}\int d\Omega_s d\Omega_i \Big[&|\phi(\Omega_s,\Omega_i)|^2 + |\phi(\Omega_i,\Omega_s)|^2 + \phi(\Omega_s,\Omega_i) \\ &\times \phi^*(\Omega_i,\Omega_s) + \phi^*(\Omega_s,\Omega_i)\phi(\Omega_i,\Omega_s) \Big] \\ &\times \{1 + \cos[(\Omega_s + \Omega_i + 2\omega_0)\tau]\}, \end{aligned} \tag{5}$$

with $R_+(\tau)$, $R_-(\tau)$, and $R_N(\tau)$ describing the coincidence-count rate for the single-port, two-port, and the N00N-state configurations, respectively. The function $\phi(\Omega_s, \Omega_i)$ represents the signal (s)-idler (i) joint spectral amplitude. The photon-pair state after interacting with the sample can be written, without loss of generality, as $|\psi\rangle = \int d\Omega_s\, d\Omega_i \phi(\Omega_s,\Omega_i)\hat{a}^\dagger(\Omega_s+\omega_0)\hat{a}^\dagger(\Omega_i+\omega_0)|0\rangle$. In writing Eqs. (4) and (5), we have assumed that the photon pairs are frequency degenerate, with a central frequency ω_0. Their frequency deviations from ω_0 are, thus, given by $\Omega_j = \omega_j - \omega_0$ ($j = s, i$). Moreover, note that we have introduced an external delay in one of the input ports of the BS. This delay allows us to perform a Hong–Ou–Mandel-like measurement on those photon pairs that are not absorbed by the sample. Interestingly, as we will describe below, the coincidence rate as a function of delay carries important information regarding the nature of the photon-pair losses.

B. ETPA as a two-photon spectral filter

Since its conception, eTPA has been described as a process in which correlated photon pairs satisfying the so-called two-photon resonance condition[14,28,37] are lost in order to drive a two-photon excitation of the absorbing medium. This means that the sample effectively acts as a *frequency filter* that removes specific resonance frequencies, thus modifying the joint spectral intensity (JSI) that characterizes the photon pairs. Mathematically, this transformation can be described by[51]

$$S(\Omega_s,\Omega_i) = |\phi(\Omega_s,\Omega_i)|^2 = |f_{\text{TP}}(\Omega_s,\Omega_i)\Phi(\Omega_s,\Omega_i)|^2, \tag{6}$$

where $\Phi(\Omega_s,\Omega_i)$ and $\phi(\Omega_s,\Omega_i)$ stand for the joint amplitude of the photons before and after the interaction with the sample, respectively. The two-photon filter can be readily defined as

$$f_{\text{TP}}(\Omega_s,\Omega_i) = 1 - \exp\left[-(\Omega_s+\Omega_i)^2/(2\sigma_{TP}^2)\right], \tag{7}$$

with σ_{TP} describing the two-photon filter bandwidth. Note that, as pointed out by Schlawin and Buchleitner,[21] the diagonal approximation of eTPA is valid, provided that the intermediate states that contribute to the two-photon excitation of the sample are located below

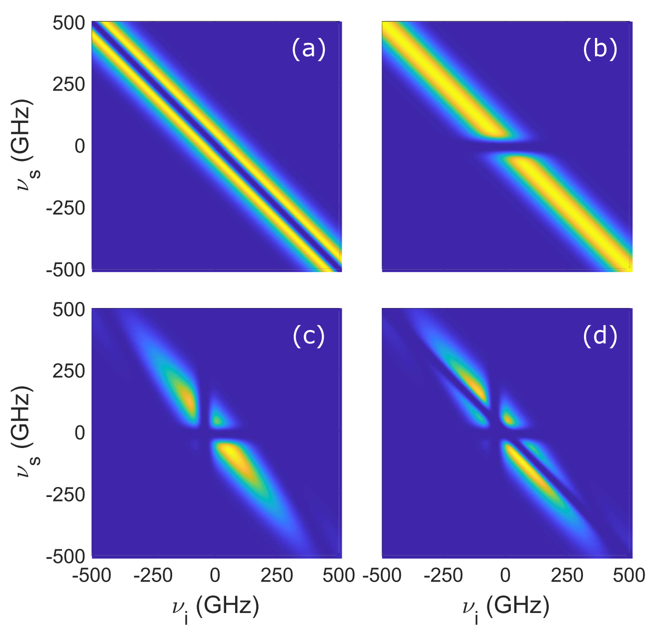

FIG. 2. Filtered joint spectral intensities (JSIs). (a) and (b) Symmetric ($\mathcal{N}_s = \mathcal{N}_i$) JSIs modified by two-photon and single-photon filters, respectively. (c) and (d) Asymmetric ($\mathcal{N}_s \neq \mathcal{N}_i$) JSIs modified by a single-photon filter in each mode and a combination of all (two-photon and single-photon) filters, respectively. Note that two-photon losses are depicted by regions along the anti-diagonal [see (a)] of the JSI, whereas single-photon losses [(b) and (c)] correspond to horizontal and vertical lines for the signal and idler modes. For the symmetric JSIs, we use $\mathcal{N}_s L = \mathcal{N}_i L = T_p$, whereas for the asymmetric case, $\mathcal{N}_s L = \mathcal{N}_i L/2 = T_p$. In all cases, we set $T_p = 5$ ps ($\sigma_p = 100$ GHz) and $\sigma_{\text{TP}} = \sigma_s = \sigma_i = 20$ GHz.

the degenerate frequency of the photon pairs—a situation found, for instance, in tetraphenylporphyrin (H_2TPP)[13]—and that the lifetime of the doubly excited state is longer than the intermediate states.

As previously discussed, in realistic experiments, the two-photon beam may experience single-photon losses (whether at the sample or elsewhere in the setup) that remove, independently, signal or idler photons. These losses can then be accounted for by writing a single-photon filter of the form

$$f_{s,i}(\Omega_s, \Omega_i) = 1 - \exp\Big[-\big(\Omega_{s,i} - \Omega_{s,i}^0\big)^2 / \big(2\sigma_{s,i}^2\big)\Big]. \tag{8}$$

Here, $\Omega_{s,i}^0$ describes the central frequency deviations of the filter, whereas $\sigma_{s,i}$ represents the single-photon filter bandwidth for the signal and idler modes, respectively. To understand the effects of the single- and two-photon filters, we assume the most general form for the initial joint spectral intensity (JSI) of the photons (see the supplementary material for details),

$$\Phi(\Omega_s, \Omega_i) = E_p(\Omega_s, \Omega_i)\mathrm{sinc}[L(\mathcal{N}_s\Omega_s + \mathcal{N}_i\Omega_i)/2] \times \exp[-iL(\mathcal{N}_s\Omega_s + \mathcal{N}_i\Omega_i)/2]. \tag{9}$$

In writing Eq. (9), we have used the definition $\mathrm{sinc}(x) = \sin(x)/x$. $E_p(\Omega_s, \Omega_i) = \exp\big[-2T_p^2(\Omega_s + \Omega_i)^2\big]$ corresponds to the Gaussian spectral shape of the classical pulsed pump, with a temporal duration T_p, which pumps the SPDC crystal of length L. Finally, $\mathcal{N}_{s,i} = k_p' - k_{s,i}'$ describes the difference between the inverse group velocity of the pump and the signal and idler photons.

Figure 2 shows some examples of filtered JSIs for (a) and (b) symmetric (resulting from type 0 or 1 SPDC with $\mathcal{N}_s = \mathcal{N}_i$) and (c) and (d) asymmetric (obtained from type-II SPDC with $\mathcal{N}_s \neq \mathcal{N}_i$) initial two-photon states. Note that two-photon losses [Fig. 2(a)] are characterized by regions along the anti-diagonal of the JSI, whereas single-photon losses [Figs. 2(b) and 2(c)] correspond to regions along the horizontal or vertical lines for the signal and idler modes.

C. Two-photon coincidence rates in the presence of one- and two-photon losses

Having defined the specific form of the two-photon state following the interaction with the sample—where one- and two-photon-loss processes may be taking place—we are now ready to evaluate the coincidence rates for each of the previously described interferometric schemes. Here, we consider three cases: (i) no filter applied, (ii) a two-photon (eTPA) filter applied, and (iii) a linear filter applied to the idler photon. While other possible cases (including a linear filter applied to both photons and the application of both linear and nonlinear filters) were considered in our analysis, they do not contribute key, additional physical insights and were, thus, omitted from the presented results.

Figure 3 shows the coincidence rate as a function of delay τ for the [(a) and (d)] single-port, [(b) and (e)] two-port, and [(c) and (f)]

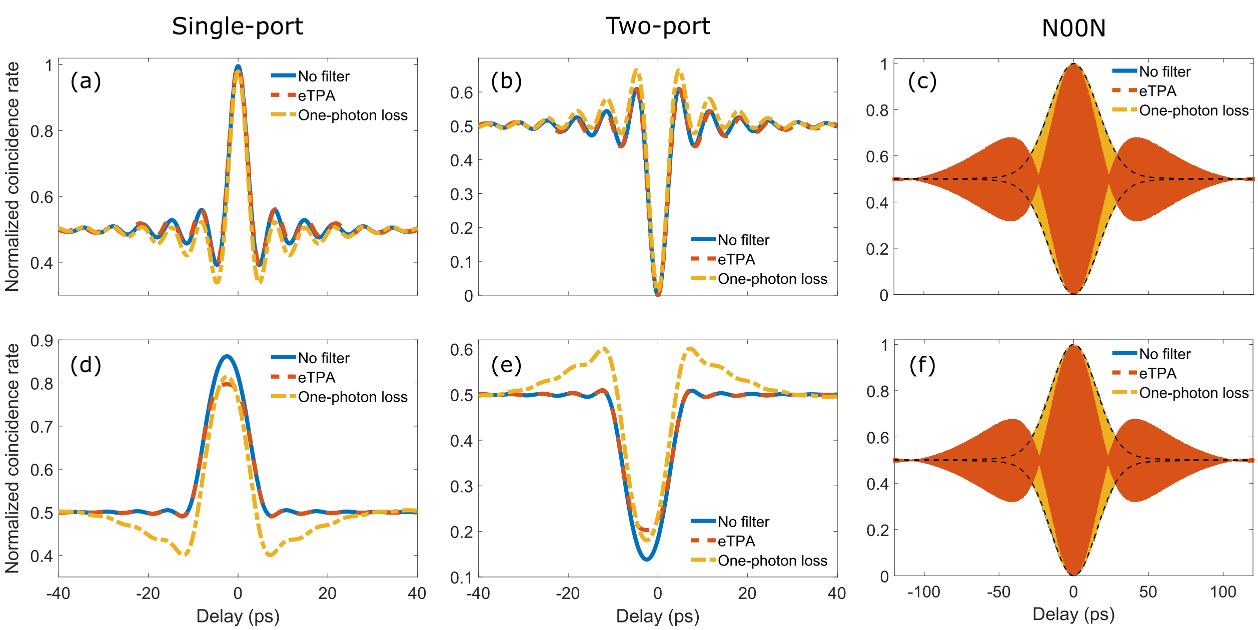

FIG. 3. Coincidence rates as a function of delay, τ, for the [(a) and (d)] single-port, [(b) and (e)] two-port, and [(c) and (f)] N00N-state configurations. The upper row shows the results for the symmetric ($\mathcal{N}_s = \mathcal{N}_i$) two-photon states, whereas the bottom row shows the results for the asymmetric ($\mathcal{N}_s \neq \mathcal{N}_i$) two-photon states. Note that for the N00N-state configuration, the no-filter measurement (blue solid line) and the one-photon loss (yellow dashed-dotted line) curves are essentially fully overlapped, while the eTPA curve (red dashed line) shows an altogether different behavior. This implies that for the symmetric or asymmetric two-photon states, the only scheme among those considered that is capable of witnessing pure eTPA is the N00N-state configuration. For the symmetric case, we have set $\mathcal{N}_sL = \mathcal{N}_iL = T_p$, while for the asymmetric case, we use $\mathcal{N}_sL = \mathcal{N}_iL/2 = T_p$. In all cases, we set $T_p = 5$ ps ($\sigma_p = 100$ GHz) and $\sigma_{TP} = \sigma_s = \sigma_i = 20$ GHz. Note that the x-axis scale for (c) and (f) is larger than that of (a) and (b) and (d) and (e). For the sake of clarity, and because the no-filter and one-photon-loss signals overlap in (c) and (f), we have included a black-dashed line depicting their envelope.

N00N-state configurations. The top row shows the results for the initially symmetric ($\mathcal{N}_s = \mathcal{N}_i$) two-photon states, whereas the bottom row shows the results for the initially asymmetric ($\mathcal{N}_s \neq \mathcal{N}_i$) states. For the symmetric case in the single- and two-port configurations, note that the no-filter (blue solid line) and eTPA (dashed red line) curves are fully overlapped, with the linear losses curve nearly overlapped with the other two, implying that one would be unable to determine the presence or absence of an eTPA sample from a transmission-based measurement. In striking contrast, for the N00N-state configuration, while the no-filter and linear filter curves are fully overlapped, the eTPA curve clearly deviates from the other two. This means that for symmetric two-photon states, the only scheme that is capable of witnessing eTPA is, indeed, the N00N-state configuration.

Let us now turn to the asymmetric case (bottom row of Fig. 3). Note that both the two-photon (eTPA) and single photon filter curves exhibit differences with the no-filter curve. Nevertheless, because the two effects occur together, broadly with a similar behavior, one may be unable to distinguish eTPA from single-photon losses by monitoring changes in the coincidence peak/dip. It is worth mentioning that in Fig. 3, the bandwidths of the one- and two-photon loss filters are assumed to be the same. Of course, if one were to suppress single photon losses, e.g., through a considerable reduction in the single photon filter bandwidth, the resulting curve would more closely follow the no-filter curve, thus allowing one to discern the presence of the eTPA process. This case may, however, not be realizable as, in practice, it is challenging to reliably ensure the absence of linear losses. Remarkably, in the N00N-state configuration once again, the single-photon loss follows the no-filter signal, whereas eTPA clearly shows an altogether different behavior. In Figs. 3(c) and 3(f), the black-dashed line depicts the envelope of the interference pattern for the no-filter and one-photon-loss signals. Note that for the N00N configuration, on the one hand, the central lobe becomes narrower and, on the other hand, additional sidelobes appear. This non-trivial interference pattern is a result of the loss of frequencies in the JSI as a result of the two-photon interaction with the sample.[57] An interesting point to note in Figs. 3(d) and 3(e) is that the dip/peak is displaced from $\tau = 0$ due to the asymmetry of the JSI [Eq. (9)]. By numerically analyzing the photon-coincidence rate for different values of $\mathcal{N}_s$ and $\mathcal{N}_i$, one can find that the single-port and two-port coincidence rates for asymmetric two-photon states will exhibit a $(\mathcal{N}_s - \mathcal{N}_i)L/2$ temporal delay shift.

In general, the HOM visibility is unity for a perfectly symmetric JSI (upon the interchange of frequency arguments), while any asymmetry results in a reduction in visibility. Note that the visibility obtained in the single- and double-port configurations, in all of the cases considered above, may be understood in terms of the symmetry properties of the resulting overall JSI, including the effect of any single-photon or two-photon filters. We would like to point out that the above-discussed results are equivalent to those obtained when the BS reflection and transmission coefficients are frequency-dependent (see the supplementary material for details). Finally, we would like to remark that the N00N-state interferometry represents a transmission-based ETPA witness. However, we could expand our ETPA-certification toolbox by investigating equivalent fluorescence-based schemes, such as two-photon Ramsey interferometers.[58–61]

III. CONCLUSION

In summary, we have explored three distinct two-photon quantum interferometers that may be used to experimentally certify true eTPA. Remarkably, we have found that the so-called N00N-state configuration is the only one among those considered that is insensitive to linear (single-photon) losses. This unique feature makes such a configuration a strong candidate for effectively certifying the absorption of correlated photon pairs in an arbitrary sample. Given the simplicity of the N00N-state configuration, and in contrast to other schemes for quantum technologies in which N00N states are not typically robust,[52,53] we expect them to play an important role in transmission-based quantum spectroscopy.

SUPPLEMENTARY MATERIAL

See supplementary material for (i) the explicit derivation of the coincidence rate for the three different interferometric configurations described in the main text, (ii) the derivation of the two-photon state that allows one to control the symmetry properties of the photons' JSI, and (iii) some examples of possible experimental schemes for the implementation of the two-photon interferometers discussed in the main text.

ACKNOWLEDGMENTS

This work was supported by DGAPA-UNAM under Project No. UNAM-PAPIIT IN101623. C.Y. and O.S.M.-L. acknowledge the funding from the U.S. Army Research Office under Grant No. W911NF2210088. A.B. thankfully acknowledges the support from AFOSR Grant No. FA9550-21-1-0147, from UNAM-PAPIIT Grant No. IN103521, and from CONACyT Grant No. 217559.

AUTHOR DECLARATIONS

Conflict of Interest

The authors have no conflicts to disclose.

Author Contributions

A.M.-T., S.C.-A., and F.T.-A. contributed equally to this work.

The theoretical and computational models were developed by A.M.-T., S.C.-A., C.Y., R.-B.J., O.S.M.-L., S.-H.D., A.B., and R.J.L.-M. The idea was conceived by A.B. and R.J.L.-M. The project was supervised by R.J.L.-M. All authors contributed to the preparation of the manuscript.

Áulide Martínez-Tapia: Formal analysis (equal); Investigation (equal); Methodology (equal); Writing – original draft (equal). **Samuel Corona-Aquino**: Formal analysis (equal); Investigation (equal); Methodology (equal); Writing – original draft (equal). **Freiman Triana-Arango**: Investigation (equal); Writing – review & editing (equal). **Chenglong You**: Formal analysis (equal); Investigation (equal); Methodology (equal); Writing – original draft (equal).

Rui-Bo Jin: Formal analysis (equal); Investigation (equal); Methodology (equal); Writing – original draft (equal). **Omar S. Magaña-Loaiza**: Formal analysis (equal); Investigation (equal); Methodology (equal); Writing – original draft (equal). **Shi-Hai Dong**: Formal analysis (equal); Investigation (equal); Methodology (equal); Writing – original draft (equal). **Alfred B. U'Ren**: Formal analysis (equal); Funding acquisition (equal); Investigation (equal); Methodology (equal); Writing – original draft (equal); Writing – review & editing (equal). **Roberto de J. León-Montiel**: Conceptualization (equal); Formal analysis (equal); Funding acquisition (equal); Investigation (equal); Methodology (equal); Supervision (equal); Writing – original draft (equal); Writing – review & editing (equal).

DATA AVAILABILITY

The data that support the findings of this study are available from the corresponding authors upon reasonable request.

REFERENCES

[1] R. R. Ernst, G. Bodenhausen, and A. Wokaun, *Principles of Nuclear Magnetic Resonance in One and Two Dimensions* (Clarendon Press, 1987).

[2] S. Mukamel, *Principles of Nonlinear Optical Spectroscopy* (Oxford University Press, 1995).

[3] P. Hamm and M. Zanni, *Concepts and Methods of 2D Infrared Spectroscopy* (Cambridge University Press, 2011).

[4] M. Cho, *Two-Dimensional Optical Spectroscopy* (CRC Press, 2009).

[5] J. Workman, *The Concise Handbook of Analytical Spectroscopy: Theory, Applications, and Reference Materials* (World Scientific, 2016).

[6] K. E. Dorfman, F. Schlawin, and S. Mukamel, "Nonlinear optical signals and spectroscopy with quantum light," Rev. Mod. Phys. **88**, 045008 (2016).

[7] F. Schlawin, "Entangled photon spectroscopy," J. Phys. B: At., Mol. Opt. Phys. **50**, 203001 (2017).

[8] H. Shi, Z. Zhang, S. Pirandola, and Q. Zhuang, "Entanglement-assisted absorption spectroscopy," Phys. Rev. Lett. **125**, 180502 (2020).

[9] C. S. Muñoz, G. Frascella, and F. Schlawin, "Quantum metrology of two-photon absorption," Phys. Rev. Res. **3**, 033250 (2021).

[10] P. Cutipa and M. V. Chekhova, "Bright squeezed vacuum for two-photon spectroscopy: Simultaneously high resolution in time and frequency, space and wavevector," Opt. Lett. **47**, 465–468 (2022).

[11] J. Javanainen and P. L. Gould, "Linear intensity dependence of a two-photon transition rate," Phys. Rev. A **41**, 5088–5091 (1990).

[12] B. Dayan, A. Pe'er, A. A. Friesem, and Y. Silberberg, "Nonlinear interactions with an ultrahigh flux of broadband entangled photons," Phys. Rev. Lett. **94**, 043602 (2005).

[13] D.-I. Lee and T. Goodson, "Entangled photon absorption in an organic porphyrin dendrimer," J. Phys. Chem. B **110**, 25582–25585 (2006).

[14] H.-B. Fei, B. M. Jost, S. Popescu, B. E. A. Saleh, and M. C. Teich, "Entanglement-induced two-photon transparency," Phys. Rev. Lett. **78**, 1679–1682 (1997).

[15] A. R. Guzman, M. R. Harpham, Ö. Süzer, M. M. Haley, and T. G. Goodson, "Spatial control of entangled two-photon absorption with organic chromophores," J. Am. Chem. Soc. **132**, 7840–7841 (2010).

[16] A. Muthukrishnan, G. S. Agarwal, and M. O. Scully, "Inducing disallowed two-atom transitions with temporally entangled photons," Phys. Rev. Lett. **93**, 093002 (2004).

[17] O. Roslyak and S. Mukamel, "Multidimensional pump-probe spectroscopy with entangled twin-photon states," Phys. Rev. A **79**, 063409 (2009).

[18] M. G. Raymer, A. H. Marcus, J. R. Widom, and D. L. P. Vitullo, "Entangled photon-pair two-dimensional fluorescence spectroscopy (EPP-2DFS)," J. Phys. Chem. B **117**, 15559–15575 (2013).

[19] F. Schlawin, K. E. Dorfman, and S. Mukamel, "Pump-probe spectroscopy using quantum light with two-photon coincidence detection," Phys. Rev. A **93**, 023807 (2016).

[20] F. Schalwin, K. E. Dorfman, B. P. Fingerhut, and S. Mukamel, "Suppression of population transport and control of exciton distributions by entangled photons," Nat. Commun. **4**, 1782 (2017).

[21] F. Schlawin and A. Buchleitner, "Theory of coherent control with quantum light," New J. Phys. **19**, 013009 (2017).

[22] M. Shapiro and P. Brumer, "Generation and control of chains of entangled atom-ion pairs with quantum light," Phys. Rev. Lett. **106**, 150501 (2011).

[23] M. Shapiro and P. Brumer, *Quantum Control of Molecular Processes* (Wiley-VCH, 2012).

[24] F. Schlawin, K. E. Dorfman, and S. Mukamel, "Entangled two-photon absorption spectroscopy," Acc. Chem. Res. **51**, 2207–2214 (2018).

[25] B. E. A. Saleh, B. M. Jost, H.-B. Fei, and M. C. Teich, "Entangled-photon virtual-state spectroscopy," Phys. Rev. Lett. **80**, 3483–3486 (1998).

[26] J. Kojima and Q.-V. Nguyen, "Entangled biphoton virtual-state spectroscopy of the $A^2\Sigma^+$–$X^2\Pi$ system of OH," Chem. Phys. Lett. **396**, 323–328 (2004).

[27] J. Peřina, B. E. A. Saleh, and M. C. Teich, "Multiphoton absorption cross section and virtual-state spectroscopy for the entangled *n*-photon state," Phys. Rev. A **57**, 3972–3986 (1998).

[28] R. de J. León-Montiel, J. Svozilík, L. J. Salazar-Serrano, and J. P. Torres, "Role of the spectral shape of quantum correlations in two-photon virtual-state spectroscopy," New J. Phys. **15**, 053023 (2013).

[29] H. Oka, "Efficient selective two-photon excitation by tailored quantum-correlated photons," Phys. Rev. A **81**, 063819 (2010).

[30] J. P. Villabona-Monsalve, O. Calderón-Losada, M. Nuñez Portela, and A. Valencia, "Entangled two photon absorption cross section on the 808 nm region for the common dyes zinc tetraphenylporphyrin and rhodamine B," J. Phys. Chem. A **121**, 7869–7875 (2017).

[31] O. Varnavski, B. Pinsky, and T. Goodson, "Entangled photon excited fluorescence in organic materials: An ultrafast coincidence detector," J. Phys. Chem. Lett. **8**, 388–393 (2017).

[32] H. Oka, "Enhanced vibrational-mode-selective two-step excitation using ultrabroadband frequency-entangled photons," Phys. Rev. A **97**, 063859 (2018).

[33] H. Oka, "Two-photon absorption by spectrally shaped entangled photons," Phys. Rev. A **97**, 033814 (2018).

[34] J. Svozilík, J. Peřina, and R. de J. León-Montiel, "Virtual-state spectroscopy with frequency-tailored intense entangled beams," J. Opt. Soc. Am. B **35**, 460–467 (2018).

[35] J. Svozilík, J. Peřina, and R. de J. León-Montiel, "Two-photon absorption spectroscopy using intense phase-chirped entangled beams," Chem. Phys. **510**, 54–59 (2018).

[36] R. K. Burdick, O. Varnavski, A. Molina, L. Upton, P. Zimmerman, and T. Goodson, "Predicting and controlling entangled two-photon absorption in diatomic molecules," J. Phys. Chem. A **122**, 8198–8212 (2018).

[37] R. de J. León-Montiel, J. Svozilik, J. P. Torres, and A. B. U'Ren, "Temperature-controlled entangled-photon absorption spectroscopy," Phys. Rev. Lett. **123**, 023601 (2019).

[38] S. Mukamel, M. Freyberger, W. Schleich, M. Bellini, A. Zavatta, G. Leuchs, C. Silberhorn, R. W. Boyd, L. L. Sánchez-Soto, A. Stefanov, M. Barbieri, A. Paterova, L. Krivitsky, S. Shwartz, K. Tamasaku, K. Dorfman, F. Schlawin, V. Sandoghdar, M. Raymer, A. Marcus, O. Varnavski, T. Goodson, Z.-Y. Zhou, B.-S. Shi, S. Asban, M. Scully, G. Agarwal, T. Peng, A. V. Sokolov, Z.-D. Zhang, M. S. Zubairy, I. A. Vartanyants, E. del Valle, and F. Laussy, "Roadmap on quantum light spectroscopy," J. Phys. B: At., Mol. Opt. Phys. **53**, 072002 (2020).

[39] L. Mertenskötter, K. Busch, and R. de J. León-Montiel, "Entangled two-photon absorption spectroscopy with varying pump wavelengths," J. Opt. Soc. Am. B **38**, C63–C68 (2021).

[40] M. G. Raymer, T. Landes, and A. H. Marcus, "Entangled two-photon absorption by atoms and molecules: A quantum optics tutorial," J. Chem. Phys. **155**, 081501 (2021).

[41] T. Landes, M. G. Raymer, M. Allgaier, S. Merkouche, B. J. Smith, and A. H. Marcus, "Quantifying the enhancement of two-photon absorption due to spectral-temporal entanglement," Opt. Express **29**, 20022–20033 (2021).

[42] M. G. Raymer, T. Landes, M. Allgaier, S. Merkouche, B. J. Smith, and A. H. Marcus, "How large is the quantum enhancement of two-photon absorption by time-frequency entanglement of photon pairs?," Optica **8**, 757–758 (2021).
[43] A. Mikhaylov, R. N. Wilson, K. M. Parzuchowski, M. D. Mazurek, C. H. Camp, M. J. Stevens, and R. Jimenez, "Hot-band absorption can mimic entangled two-photon absorption," J. Phys. Chem. Lett. **13**, 1489–1493 (2022).
[44] B. P. Hickam, M. He, N. Harper, S. Szoke, and S. K. Cushing, "Single-photon scattering can account for the discrepancies among entangled two-photon measurement techniques," J. Phys. Chem. Lett. **13**, 4934–4940 (2022).
[45] J. P. Villabona-Monsalve, R. K. Burdick, and T. Goodson, "Measurements of entangled two-photon absorption in organic molecules with CW-pumped type-I spontaneous parametric down-conversion," J. Phys. Chem. C **124**, 24526–24532 (2020).
[46] K. M. Parzuchowski, A. Mikhaylov, M. D. Mazurek, R. N. Wilson, D. J. Lum, T. Gerrits, C. H. Camp, M. J. Stevens, and R. Jimenez, "Setting bounds on entangled two-photon absorption cross sections in common fluorophores," Phys. Rev. Appl. **15**, 044012 (2021).
[47] D. Tabakaev, M. Montagnese, G. Haack, L. Bonacina, J.-P. Wolf, H. Zbinden, and R. T. Thew, "Energy-time-entangled two-photon molecular absorption," Phys. Rev. A **103**, 033701 (2021).
[48] T. Landes, M. Allgaier, S. Merkouche, B. J. Smith, A. H. Marcus, and M. G. Raymer, "Experimental feasibility of molecular two-photon absorption with isolated time-frequency-entangled photon pairs," Phys. Rev. Res. **3**, 033154 (2021).
[49] S. Corona-Aquino, O. Calderón-Losada, M. Y. Li-Gómez, H. Cruz-Ramírez, V. Álvarez-Venicio, M. D. P. Carreón-Castro, R. de J. León-Montiel, and A. B. U'Ren, "Experimental study of the validity of entangled two-photon absorption measurements in organic compounds," J. Phys. Chem. A **126**, 2185–2195 (2022).
[50] D. Tabakaev, A. Djorović, L. La Volpe, G. Gaulier, S. Ghosh, L. Bonacina, J.-P. Wolf, H. Zbinden, and R. T. Thew, "Spatial properties of entangled two-photon absorption," Phys. Rev. Lett. **129**, 183601 (2022).
[51] F. Triana-Arango, G. Ramos-Ortiz, and R. Ramírez-Alarcón, "Entangled two-photon absorption detection through a Hong-Ou-Mandel interferometer," http://arxiv:2202.05985 (2022).
[52] N. Thomas-Peter, B. J. Smith, A. Datta, L. Zhang, U. Dorner, and I. A. Walmsley, "Real-world quantum sensors: Evaluating resources for precision measurement," Phys. Rev. Lett. **107**, 113603 (2011).
[53] C. You, M. Hong, P. Bierhorst, A. E. Lita, S. Glancy, S. Kolthammer, E. Knill, S. W. Nam, R. P. Mirin, O. S. Magaña-Loaiza, and T. Gerrits, "Scalable multiphoton quantum metrology with neither pre- nor post-selected measurements," Appl. Phys. Rev. **8**, 041406 (2021).
[54] S. M. Barnett, J. Jeffers, A. Gatti, and R. Loudon, "Quantum optics of lossy beam splitters," Phys. Rev. A **57**, 2134–2145 (1998).
[55] S. M. Barnett and P. M. Radmore, *Methods in Theoretical Quantum Optics* (Oxford University Press, 1997).
[56] R.-B. Jin and R. Shimizu, "Extended Wiener–Khinchin theorem for quantum spectral analysis," Optica **5**, 93–98 (2018).
[57] Y. Chen, R. de J. León-Montiel, and L. Chen, "Quantum interferometric two-photon excitation spectroscopy," New J. Phys. **24**, 113014 (2022).
[58] G. S. Agarwal and M. O. Scully, "Ramsey spectroscopy with nonclassical light sources," Phys. Rev. A **53**, 467–470 (1996).
[59] G. S. Agarwal, P. K. Pathak, and M. O. Scully, "Single-atom and two-atom Ramsey interferometry with quantized fields," Phys. Rev. A **67**, 043807 (2003).
[60] K. Qu and G. S. Agarwal, "Ramsey spectroscopy with squeezed light," Opt. Lett. **38**, 2563–2565 (2013).
[61] F. Schlawin and S. Mukamel, "Two-photon spectroscopy of excitons with entangled photons," J. Chem. Phys. **139**, 244110 (2013).